# Fano resonant all-dielectric core/shell nanoparticles with ultrahigh scattering directionality in the visible region

**Yuta Tsuchimoto,[1] Taka-aki Yano,[1,2,*] Tomohiro Hayashi,[1,2] and Masahiko Hara[1,2,3]**

[1]*School of Materials and Chemical Technology, Tokyo Institute of Technology, Yokohama, Kanagawa, 226-8503, Japan*

[2]*RIKEN, 2-1 Hirosawa, Wako, Saitama 351-0198, Japan*

[3]*Earth-Life Science Institute, Tokyo Institute of Technology, Meguro, Tokyo 152-8551, Japan*

[*]*yano@echem.titech.ac.jp*

**Abstract:** We demonstrate Si-based single core/shell ($Si/SiO_2$) nanoparticles which exhibit the Fano resonance associated with ultrahigh scattering directionality. The $SiO_2$ shell plays a crucial role in achieving zero backscattering at the Fano resonance wavelength along with strongly-enhanced forward scattering. As a result, the front-to-back scattering-intensity ratio is five orders of magnitude greater than that of a Si nanoparticle. Furthermore, the Fano resonance wavelength is controlled over the entire visible region by changing the core diameter. The Fano spectra also show distinctive intensity modulations depending on the index of refraction of the surrounding medium. These unique features make $Si/SiO_2$ nanoparticles promising for the design of low-loss nano-antennas, metamaterials, and other nanophotonic devices.

©2016 Optical Society of America

**OCIS codes:** (290.0290) Scattering; (310.6628) Subwavelength structures, nanostructures.

## References and links

1. M. Tomita, K. Totsuka, R. Hanamura, and T. Matsumoto, "Tunable Fano interference effect in coupled-microsphere resonator-induced transparency," J. Opt. Soc. Am. **26**(4), 813–818 (2009).
2. B. Luk'yanchuk, N. I. Zheludev, S. A. Maier, N. J. Halas, P. Nordlander, H. Giessen, and C. T. Chong, "The Fano resonance in plasmonic nanostructures and metamaterials," Nat. Mater. **9**(9), 707–715 (2010).
3. N. Papasimakis and N. I. Zheludev, "Metamaterial-induced transparency: sharp Fano resonances and slow light," Opt. Photonics News **20**(10), 22–27 (2009).
4. C. Chao and L. J. Guo, "Biochemical sensors based on polymer microrings with sharp asymmetrical resonance," Appl. Phys. Lett. **83**(8), 1527 (2016).
5. W. S. Chang, J. B. Lassiter, P. Swanglap, H. Sobhani, S. Khatua, P. Nordlander, N. J. Halas, and S. Link, "A plasmonic Fano switch," Nano Lett. **12**(9), 4977–4982 (2012).
6. T. Pakizeh and M. Käll, "Unidirectional ultracompact optical nanoantennas," Nano Lett. **9**(6), 2343–2349 (2009).
7. K. E. Chong, B. Hopkins, I. Staude, A. E. Miroshnichenko, J. Dominguez, M. Decker, D. N. Neshev, I. Brener, and Y. S. Kivshar, "Observation of Fano resonances in all-dielectric nanoparticle oligomers," Small **10**(10), 1985–1990 (2014).
8. Z. Jia, J. Li, H. Wu, C. Wang, T. Chen, R. Peng, and M. Wang, "Dipole coupling and dual Fano resonances in a silicon nanodimer," J. Appl. Phys. **119**(7), 074302 (2016).
9. A. E. Miroshnichenko and Y. S. Kivshar, "Fano resonances in all-dielectric oligomers," Nano Lett. **12**(12), 6459–6463 (2012).
10. J. Yan, P. Liu, Z. Lin, H. Wang, H. Chen, C. Wang, and G. Yang, "Directional Fano resonance in a silicon nanosphere dimer," ACS Nano **9**(3), 2968–2980 (2015).
11. D.-J. Cai, Y.-H. Huang, W.-J. Wang, W.-B. Ji, J.-D. Chen, Z.-H. Chen, and S.-D. Liu, "Fano resonances generated in a single dielectric homogeneous nanoparticle with high structural symmetry," J. Phys. Chem. C **119**(8), 4252–4260 (2015).
12. W. Zhao, D. Ju, Y. Jiang, and Q. Zhan, "Dipole and quadrupole trapped modes within bi-periodic silicon particle array realizing three-channel refractive sensing," Opt. Express **22**(25), 31277–31285 (2014).
13. M. V. Rybin, P. V. Kapitanova, D. S. Filonov, A. P. Slobozhanyuk, P. A. Belov, Y. S. Kivshar, and M. F. Limonov, "Fano resonances in antennas: general control over radiation patterns," Phys. Rev. B **88**(20), 205106 (2013).
14. P. Fan, Z. Yu, S. Fan, and M. L. Brongersma, "Optical Fano resonance of an individual semiconductor nanostructure," Nat. Mater. **13**(5), 471–475 (2014).

#262908 Received 12 Apr 2016; revised 14 Jun 2016; accepted 15 Jun 2016; published 17 Jun 2016
© 2016 OSA

15. J. C. Ginn, I. Brener, D. W. Peters, J. R. Wendt, J. O. Stevens, P. F. Hines, L. I. Basilio, L. K. Warne, J. F. Ihlefeld, P. G. Clem, and M. B. Sinclair, "Realizing optical magnetism from dielectric metamaterials," Phys. Rev. Lett. **108**(9), 097402 (2012).
16. A. I. Kuznetsov, A. E. Miroshnichenko, Y. H. Fu, J. Zhang, and B. Luk'yanchuk, "Magnetic light," Sci. Rep. **2**, 492 (2012).
17. A. B. Evlyukhin, S. M. Novikov, U. Zywietz, R. L. Eriksen, C. Reinhardt, S. I. Bozhevolnyi, and B. N. Chichkov, "Demonstration of magnetic dipole resonances of dielectric nanospheres in the visible region," Nano Lett. **12**(7), 3749–3755 (2012).
18. M. Kerker, D.-S. Wang, and C. L. Giles, "Electromagnetic scattering by magnetic spheres," J. Opt. Soc. Am. **73**(6), 765–767 (1983).
19. Y. H. Fu, A. I. Kuznetsov, A. E. Miroshnichenko, Y. F. Yu, and B. Luk'yanchuk, "Directional visible light scattering by silicon nanoparticles," Nat. Commun. **4**, 1527 (2013).
20. S. Person, M. Jain, Z. Lapin, J. J. Sáenz, G. Wicks, and L. Novotny, "Demonstration of zero optical backscattering from single nanoparticles," Nano Lett. **13**(4), 1806–1809 (2013).
21. B. Rolly, B. Stout, and N. Bonod, "Boosting the directivity of optical antennas with magnetic and electric dipolar resonant particles," Opt. Express **20**(18), 20376–20386 (2012).
22. A. E. Krasnok, A. E. Miroshnichenko, P. A. Belov, and Y. S. Kivshar, "All-dielectric optical nanoantennas," Opt. Express **20**(18), 20599–20604 (2012).
23. I. Staude, A. E. Miroshnichenko, M. Decker, N. T. Fofang, S. Liu, E. Gonzales, J. Dominguez, T. S. Luk, D. N. Neshev, I. Brener, and Y. Kivshar, "Tailoring directional scattering through magnetic and electric resonances in subwavelength silicon nanodisks," ACS Nano **7**(9), 7824–7832 (2013).
24. P. Albella, T. Shibanuma, and S. A. Maier, "Switchable directional scattering of electromagnetic radiation with subwavelength asymmetric silicon dimers," Sci. Rep. **5**, 18322 (2015).
25. H. Wang, P. Liu, Y. Ke, Y. Su, L. Zhang, N. Xu, S. Deng, and H. Chen, "Janus magneto-electric nanosphere dimers exhibiting unidirectional visible light scattering and strong electromagnetic field enhancement," ACS Nano **9**(1), 436–448 (2015).
26. J. M. Geffrin, B. García-Cámara, R. Gómez-Medina, P. Albella, L. S. Froufe-Pérez, C. Eyraud, A. Litman, R. Vaillon, F. González, M. Nieto-Vesperinas, J. J. Sáenz, and F. Moreno, "Magnetic and electric coherence in forward- and back-scattered electromagnetic waves by a single dielectric subwavelength sphere," Nat. Commun. **3**, 1171 (2012).
27. B. S. Luk'yanchuk, A. E. Miroshnichenko, and Y. S. Kivshar, "Fano resonances and topological optics: an interplay of far- and near-field interference phenomena," J. Opt. **15**(7), 073001 (2013).
28. K. V. Baryshnikova, M. I. Petrov, V. E. Babicheva, and P. A. Belov, "Plasmonic and silicon spherical nanoparticle antireflective coatings," Sci. Rep. **6**, 22136 (2016).
29. Y. Yang, I. I. Kravchenko, D. P. Briggs, and J. Valentine, "All-dielectric metasurface analogue of electromagnetically induced transparency," Nat. Commun. **5**, 5753 (2014).
30. R. R. Naraghi, S. Sukhov, and A. Dogariu, "Directional control of scattering by all-dielectric core-shell spheres," Opt. Lett. **40**(4), 585–588 (2015).
31. Y. Tsuchimoto, T. A. Yano, M. Hada, K. G. Nakamura, T. Hayashi, and M. Hara, "Controlling the visible electromagnetic resonances of $Si/SiO_2$ dielectric core-shell nanoparticles by thermal oxidation," Small **11**(37), 4844–4849 (2015).
32. A. E. Miroshnichenko, S. Flach, and Y. S. Kivshar, "Fano resonances in nanoscale structures," Rev. Mod. Phys. **82**(3), 2257–2298 (2010).
33. E. D. Palik, *Handbook of Optical Constants of Solids* (Academic, 1985).
34. C. F. Bohren and D. R. Huffman, *Absorption and Scattering of Light by Small Particles* (John Wiley and Sons, 1983).
35. W. Liu, A. E. Miroshnichenko, D. N. Neshev, and Y. S. Kivshar, "Broadband unidirectional scattering by magneto-electric core-shell nanoparticles," ACS Nano **6**(6), 5489–5497 (2012).
36. Y. Li, M. Wan, W. Wu, Z. Chen, P. Zhan, and Z. Wang, "Broadband zero-backward and near-zero-forward scattering by metallo-dielectric core-shell nanoparticles," Sci. Rep. **5**, 12491 (2015).
37. J. Yan, P. Liu, Z. Lin, and G. Yang, "New type high-index dielectric nanosensors based on the scattering intensity shift," Nanoscale **8**(11), 5996–6007 (2016).
38. B. García-Cámara, R. Gómez-Medina, J. J. Sáenz, and B. Sepúlveda, "Sensing with magnetic dipolar resonances in semiconductor nanospheres," Opt. Express **21**(20), 23007–23020 (2013).

## 1. Introduction

Fano resonance is a ubiquitous physical phenomenon that has been observed not only in quantum systems but also in classic optical systems such as high-$Q$ microspheres [1], photonic crystals, and plasmonic nanostructures [2]. In classical optics, Fano resonances result from constructive and destructive interferences between broad and narrow resonances. The unique Fano line shape and dip derived from such interferences have the potential to enable slow-light devices [3], optical sensors [4], switches [5], nano-antennas [6], etc. Recently, the Fano resonance has been observed in dielectric nanostructures with a high index of refraction and low energy losses [6–14]. Dielectric nanostructures allow us to excite not only electric dipoles (EDs) but also strong magnetic dipoles (MDs) within these structures

#262908 Received 12 Apr 2016; revised 14 Jun 2016; accepted 15 Jun 2016; published 17 Jun 2016
© 2016 OSA

[15] and thereby generate resonant scattering with low energy loss in the visible region of the spectrum [16, 17]. The fundamental characteristics of electromagnetic resonances have been thoroughly studied both experimentally and theoretically. For dielectric nanostructures, MDs have sharp and strong resonance peaks whereas EDs have relatively broad resonance peaks [10, 17]. Thus, the interference between EDs and strong MDs creates the magnetic-based Fano resonance near the magnetic resonance frequency. Si heptamers [7, 9], dimmers [10], and even single-symmetry structures [11] have been demonstrated experimentally to exhibit magnetic-based Fano resonances in the visible region.

Dielectric nanostructures provide another attractive phenomenon. In 1983, Kerker et al. predicted theoretically that the interference of electric and magnetic multipoles should give rise to directional scattering [18]. In the visible region, Kerker-type directional scattering has been demonstrated experimentally in Si nanoparticles [19]. Under the first Kerker condition, backscattered light is completely suppressed, realizing so called "zero backscattering," which has been demonstrated by using GaAs pillars [20]. Furthermore, controlling the scattering directivity has been studied in a host of systems [10, 13, 21–26], such as single nanospheres [19, 21, 26], arrays [22], nanodisks [23], and nanodimers [10, 24, 25]. Because the directional scattering of dielectric nanostructures originates from the interference between electric and magnetic multipoles, it can be associated with the Fano resonance. The Fano resonance associated with the directional scattering is called the "directional Fano resonance" [19, 27] and has recently been observed in Si nanodimers [10]. Engineering such electromagnetic interaction by dielectric nanostructures is a promising approach for fabricating low-loss optical nano-antennas [22], metamaterials [28, 29], and other nanophotonic devices.

To implement the low-loss resonant scattering phenomena and control them with precision, all-dielectric core/shell nanostructures are highly promising candidates [30, 31]. In this work, we utilize single $Si/SiO_2$ core/shell nanoparticles [31] to demonstrate a directional Fano resonance in the visible spectrum. In general, a Fano resonance leads to a resonant suppression of scattering in any direction depending on the interaction between electromagnetic resonances [2, 32]. In our system, a Fano resonance arises with suppressed backward scattering. Furthermore, enhanced forward scattering coincides with this backward suppression. In this paper, we define this Fano resonance associated with the directional scattering as a directional Fano resonance. The $SiO_2$ shell enables to realize zero backscattering at the Fano resonance wavelength along with strongly-enhanced forward scattering. The ratio of forward-scattering to backward-scattering intensity increases by five orders of magnitude with respect to that of a Si nanoparticle. In addition, we report a clear change in intensity in the Fano spectra as a function of index of refraction of the surrounding medium.

## 2. Methods

### *2.1 Sample fabrication and optical measurements*

Si nanoparticles with spherical diameters of 100–300 nm were fabricated through laser ablation by using a femtosecond laser (Hurricane, Spectra physics). In laser ablation, we used the experimental conditions described in previous studies [16, 19]. A quartz glass plate was placed parallel to a Si wafer. The distance between quartz plate and wafer was fixed at 2 mm. The pulsed laser was operated at a repetition–rate of 1 kHz. The pulse width and energy were set to 100 fs and 1 mJ, respectively, at a central wavelength of 800 nm. The laser beam was focused onto the wafer surface through the quartz plate. The diameter of the beam spot on the wafer surface spot was ~10 μm. Ablated Si nanoparticles were collected on the quartz plate. The Si nanoparticles fabricated were confirmed to be crystal as already discussed in our previous report [31], and hence dielectric constants of crystalline Si were used for the following numerical calculation. In our previous report, we have already confirmed that Si nanoparticles are crystals by comparing an experimental scattering spectrum and calculated one using dielectric constants of crystalline Si [31].

#262908 Received 12 Apr 2016; revised 14 Jun 2016; accepted 15 Jun 2016; published 17 Jun 2016
© 2016 OSA

After the temperature of an electric furnace was stabilized at 900 °C, the nanoparticles were quickly placed in the furnace. The nanoparticles were thermally oxidized in dry air so that a $SiO_2$ shell formed around each Si nanoparticle.

Fabricated core/shell nanoparticles were moved to a dark-field optical microscope (IX71, OLYMPUS), following which forward- and backward-scattered light from the individual nanoparticles was measured. Figure 1 shows a schematic of our experimental set-up. A halogen lamp served as light source. For forward-scattering measurements, the light was incident on the samples through a dark-field condenser (NA = 0.7–0.9), which led to an angle of incidence between 44° and 64° with respect to the normal to the quartz substrate. The forward-scattered light was collected by an objective (SLCPlanFL, OLYMPUS, NA = 0.55, 40X), which provided a total angle for light collection of 67°. For backward-scattering measurements, the incident light was focused on a corner at the back focal plane of the objective, and then collimated light was incident on the sample at 33° with respect to the normal to the quartz substrate. Backward-scattered and reflected light was collected by the same objective. Here, scattered light with high scattering angle and reflected light was cut out by introducing a mask shading half of the pupil surface of the objective. Finally, light scattered in the range of 0°–33° emerged from the objective. For both forward- and backward-scattering measurements, the collected light was detected by using a spectrometer (IsoPlane SCT160, Princeton Instruments) equipped with an EMCCD (ProEM512, Princeton Instruments). By alternately repeating the thermal oxidation and dark-field observation for a given sample, scattering spectra from given nanoparticles with different core/shell ratios were obtained.

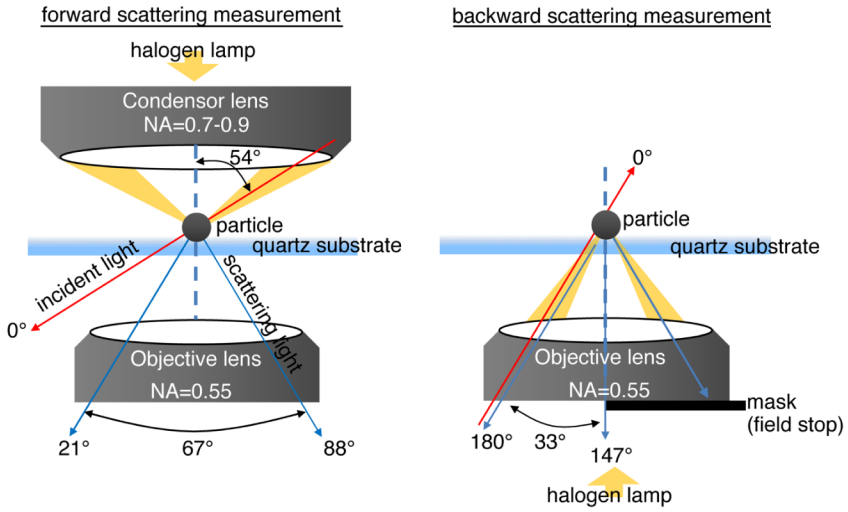


Fig. 1. Schematics of forward- and backward-scattering measurements.

### *2.2 Calculations*

For numerical analysis of electromagnetic responses, we used the finite element method software package COMSOL Multiphysics 4.4 (COMSOL Inc., Burlington, MA, USA). In the calculations, a single spherical $Si/SiO_2$ nanoparticle or a bare Si nanoparticle in air were assumed. A plane wave was incident on the particle, and then forward and backward scattered light were collected over the angle range of 21°-88° and 0°-33° from the incident axis. These detection ranges correspond to the experimental ones shown in the Fig. 1. The presence of the substrate in our experiments was neglected because the quartz substrate does not affect scattering directionality largely. The dielectric constants of Si and $SiO_2$ were taken from Palik [33] and we assumed crystalline Si in our calculations.

#262908 Received 12 Apr 2016; revised 14 Jun 2016; accepted 15 Jun 2016; published 17 Jun 2016
© 2016 OSA

Mie theory was used to calculate scattering cross sections and forward- and backward-scattering intensities for various $Si/SiO_2$ and Si nanoparticles. Scattering cross sections of single homogeneous spheres or core/shell spheres are given by

$$C_{scat} = \frac{2\pi}{k^2}\sum_n (2n+1)\left(|a_n|^2 + |b_n|^2\right) \quad (1)$$

where $k$ is the wave number, $a_n$ and $b_n$ are the electric and magnetic Mie coefficients, and $n$ is the order of the multipole moments: $n$ = 1 and 2 indicate dipole and quadrupole moments, respectively [34]. Backward- and forward-scattering intensities are defined as

$$I_B = \left(\frac{1}{4k^2}\right)\left|\sum_n (2n+1)(-1)^n (a_n - b_n)\right|^2 \quad (2)$$

$$I_F = \left(\frac{1}{4k^2}\right)\left|\sum_n (2n+1)(a_n + b_n)\right|^2 \quad (3)$$

respectively, where $I_B$ and $I_F$ are normalized to the incident intensity [18, 26, 35]. The calculations included terms up to order ~10.

## 3. Results and discussion

First, we report experimental and numerically calculated results that indicate that forming a $SiO_2$ shell around a Si core generates a directional Fano resonance. To clearly understand the role of the $SiO_2$ shell in this directional Fano resonance, we compared a Si nanoparticle with a $Si/SiO_2$ nanoparticle with the same Si-core diameter. Figure 2(a) shows a scanning electron microscope (SEM) image of a Si nanoparticle fabricated by laser ablation, confirming that the particle diameter is approximately 130 nm. Backward- and forward-scattering spectra of the particle are shown in the Figs. 2(b) and 2(c), respectively. Experimental and calculated spectra (solid and dashed line) are displayed together in each figure. For both backward and forward scattering spectra, the experimental spectrum shows clear resonance peaks originating from ED and MD resonances at the wavelengths of 470 and 550 nm respectively. These spectral shapes are consistent with those of previous reports [17, 19]. The calculated spectra of a Si nanoparticle with a diameter of 134 nm are well consistent with the experimental one. Deviations of resonant wavelengths and intensities between these spectra arise from the distorted particle shape in the experiment and the dressing effect because of the substrate [16, 19]. Figure 2(d) displays an SEM image of a $Si/SiO_2$ nanoparticle taken at the accelerating voltage of 15 kV. A core/shell structure can be seen as an intensity contrast originating from the difference of secondary electron emission yield as already reported in our previous report [31]. From this image, the core diameter and shell thickness were estimated to be 130 and 75 nm, respectively, which were used in the numerical calculation. Backward- and forward-scattering spectra of the $Si/SiO_2$ nanoparticle are shown in Figs. 2(e) and 2(f), respectively. Experimental and calculated spectra are again displayed together in each figure. For the backward-scattering spectra, the scattering intensity at longer wavelengths (>600 nm) is enhanced compared with that of the Si nanoparticle. As a result, an asymmetric Fano lineshape appears and a distinct dip structure is generated. The reason why the experimental one shows a clearer dip structure than the calculated one is attributed to small resonant wavelength difference between the MD and ED due to the distorted particle shape [19]. When it comes to the forward-scattering spectra, strong scattering intensity occurs at the wavelength corresponding to the dip in the backward-scattering spectra. This result demonstrates that a directional Fano resonance occurs in $Si/SiO_2$ core/shell nanoparticles.

#262908 Received 12 Apr 2016; revised 14 Jun 2016; accepted 15 Jun 2016; published 17 Jun 2016
© 2016 OSA

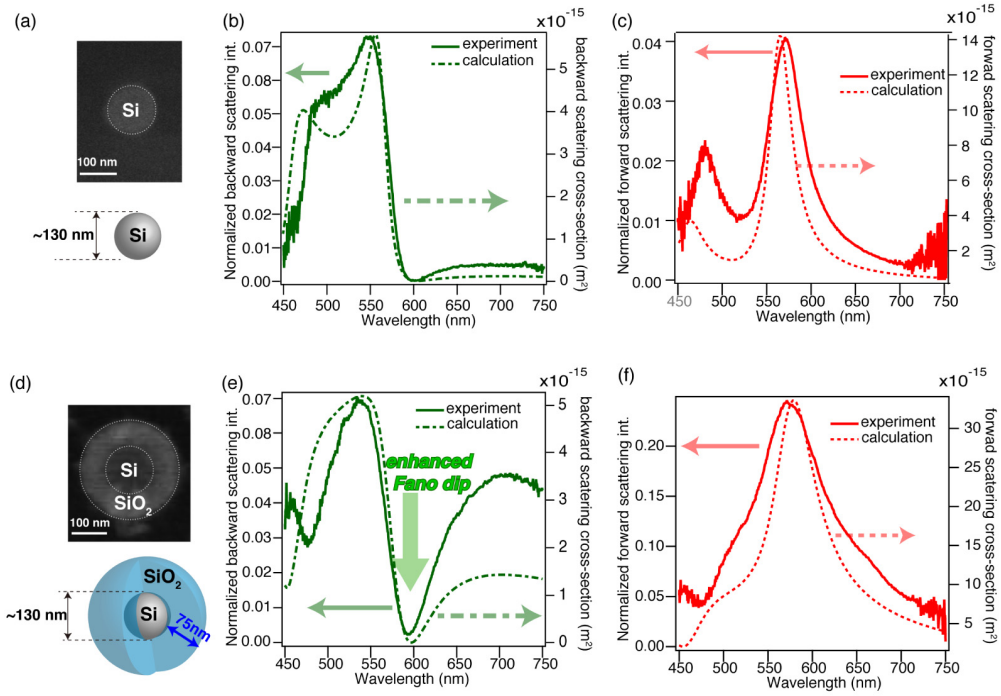


Fig. 2. Backward-scattering (green curve) spectra and forward-scattering (red curve). (a) SEM image and schematic of a Si nanoparticle. The scale bar shows 100 nm. (b), (c) backward- and forward-scattering spectra of the Si nanoparticle. Solid and dashed lines indicate experimental and calculated results, respectively. (d) SEM image and schematic of a $Si/SiO_2$ nanoparticle. (e), (f) backward- and forward-scattering spectra of the $Si/SiO_2$ nanoparticle.

To reveal the origin of the Fano resonance in this system, we applied a dipole analysis [10] based on Mie theory. Since quadrupole resonances are located out of the visible region, only dipole components were taken into consideration. Scattering cross sections of ED and MD resonances were calculated for Si and $Si/SiO_2$ nanoparticles. The diameter of the Si nanoparticle was again 130 nm, and the core diameter and shell thickness of the $Si/SiO_2$ nanoparticle were again 130 and 75 nm, respectively. Figure 3(a) shows scattering cross sections of ED and MD components for the Si nanoparticle. Peaks originating from the electric and magnetic resonances appear at 460 and 550 nm, respectively. The peaks are separated from each other, so that superposition between the two dipole components is small. For the $Si/SiO_2$ nanoparticle [Fig. 3(b)], the peaks appear at 520 and 580 nm, which are separated less than the Si nanoparticle peaks. Furthermore, the ED resonance is much broader than the Si nanoparticle, whereas the width of the magnetic resonance is almost the same as that of the Si nanoparticle. Thus, the broad ED and relatively narrow MD resonances interact with each other to generate the clear magnetic-based Fano resonance in the $Si/SiO_2$ nanoparticle.

We now discuss what broadens the ED resonance in this system. Note that the difference is large between the indices of refraction of the Si surfaces of bare Si and $Si/SiO_2$ nanoparticles in air. First, we verified whether the origin of the broad ED resonance in this system may be attributed to a homogeneous change in the index of refraction of the medium surrounding the Si surface. Figure 3(c) displays the calculated scattering cross sections of the ED resonant components for different three types: Type 1 is a Si nanoparticle (diameter of 130 nm) in air, Type 2 is a Si nanoparticle (diameter of 130 nm) in a medium with index of refraction of 1.45 (the same as the index of refraction of $SiO_2$), and Type 3 is a $Si/SiO_2$ nanoparticle (core diameter is 130 nm, shell thickness is 75 nm) in air. The spectra were normalized by their maximum intensity. For Type 1, the ED component exhibits a narrow

#262908 Received 12 Apr 2016; revised 14 Jun 2016; accepted 15 Jun 2016; published 17 Jun 2016
© 2016 OSA

resonance peak around λ = 460 nm, as also seen in Fig. 3(a). When the surrounding index of refraction changes to 1.45 (Type 2), the ED resonance becomes broader than that of Type 1, indicating that the homogeneous change in the surrounding index of refraction broadens the ED resonance. This result is attributed to the confinement of the electric near field being weakened because of the relatively small difference in index of refraction between the Si surface and the surrounding medium. The broadening of the ED resonance, however, is much less than that for Type 3. The result shown in Fig. 3(d) indicates that the origin of the broad ED resonance cannot be explained only by the homogeneous change in the index of refraction of the surrounding medium, which means that forming a $SiO_2$ shell around the core is indispensable to the broad ED resonance.

In the case of homogeneous particles such as Si nanoparticles, directional scattering occurs in an off-resonant regime [19], which does not allow us to see a directional Fano resonance. On the other hand, the $Si/SiO_2$ nanoparticle shows the directional scattering in an on-resonant regime [Fig. 2(e) and 2(f)]. Here, we discuss the reason why the directional scattering appears in the on-resonant regime. A possible reason is red-shift of the MD resonance due to the forming of a $SiO_2$ shell. Figure 3(e) exhibits wavelengths of the MD resonance and the Fano dip in backward-scattering spectra calculated by the Mie theory as a function of the shell thickness. One can clearly see that the MD resonant wavelength shifts to the longer wavelength side as increasing the shell thickness. This red-shift reduces the wavelength difference between the MD resonance and dip from 41 to 17 nm, making the dip overlapped with the MD resonant regime. This result implies that the red-shift of the MD resonance due to the forming a $SiO_2$ shell leads the directional scattering in the on-resonant regime.

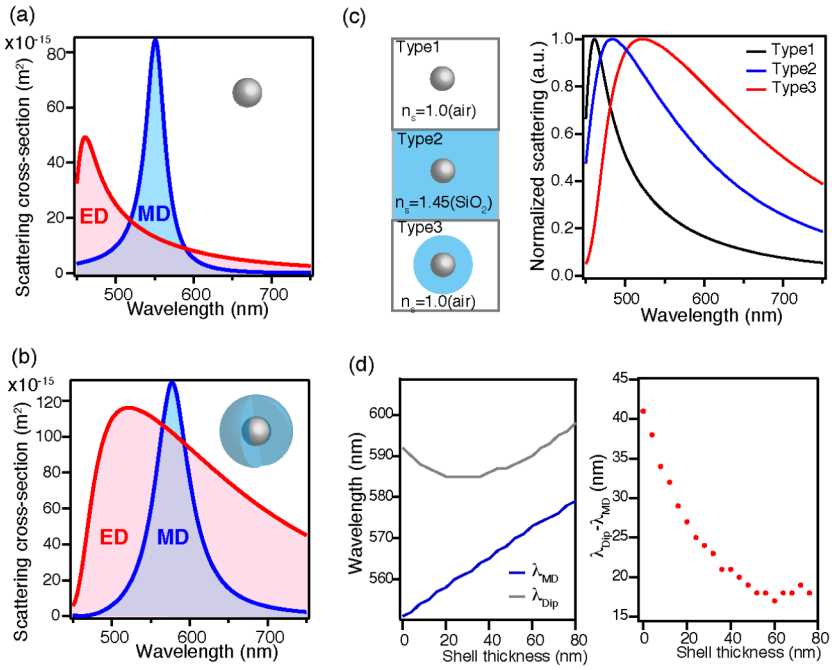


Fig. 3. (a), (b) Scattering cross sections of ED (red curve) and MD (blue curve) components for (a) Si and (b) $Si/SiO_2$ nanoparticles. The diameter of the Si nanoparticle and of the Si core is 130 nm and the $SiO_2$ shell is 75 nm thick. (c) Calculated scattering cross sections of ED resonances for the Si and $Si/SiO_2$ nanoparticles in various surrounding media. The black and blue lines indicate the spectra for the Si nanoparticle in a surrounding medium with index of refraction of 1.0 and 1.45, respectively. The red line shows the spectra for the $Si/SiO_2$ nanoparticle in a surrounding medium with index of refraction of 1.0. (d) Shell thickness dependence of wavelengths of the Fano dip and MD resonance. The left and right graphs show the absolute wavelengths and its difference, respectively.

#262908 Received 12 Apr 2016; revised 14 Jun 2016; accepted 15 Jun 2016; published 17 Jun 2016
© 2016 OSA

The influence of the shell thickness on the Fano resonance and directional scattering was investigated both experimentally and theoretically. Figure 4(a) shows schematics of a Si nanoparticle and $Si/SiO_2$ nanoparticles with approximately the same Si-core diameters (~130 nm) and various $SiO_2$ shell thicknesses (0, 35, and 75 nm). Figures 4(b) and 4(c) show experimental backward- and forward-scattering spectra from those nanoparticles. Samples of each type of particle were fabricated by thermal oxidation for 0, 180, and 240 min. For the backward-scattering spectra, when the $SiO_2$ shell is not present, peaks attributed to the ED and MD resonances appear separately at $\lambda$ = 490 and 545 nm, respectively. The intensity at wavelengths greater than 600 nm is drastically enhanced with increasing shell thickness. When the shell thickness exceeds ~40 nm, the clear Fano dip appears. For the forward-scattering spectra, the intensity increases over the entire visible wavelength region as the $SiO_2$ shell gets thicker. In particular, for the wavelength corresponding to that of the Fano dip, the forward-scattering intensity for the 75-nm-thick shell increases 13-fold compared with the forward-scattering intensity for the particles with no $SiO_2$ shell, whereas the backward-scattering intensity remains nearly zero.

Figures 4(d) and 4(e) show color maps of numerically calculated backward and forward scattering spectra for $Si/SiO_2$ nanoparticles with a fixed core diameter of 130 nm and a shell thickness that varies from 0 to 100 nm. In Fig. 4(d), the yellow region located below $\lambda$ = 580 nm is assigned to the ED and MD modes. The black region located near $\lambda$ = 590 nm indicates the dip originating from the Fano resonance. The intensity at wavelengths greater than 600 nm gradually increases with increasing shell thickness. The distinctive Fano dip appears for thicknesses greater than ~40 nm. In contrast to the backward-scattering intensity, the forward-scattering intensity shown in Fig. 4(e) continues rising with increasing shell thickness. At the wavelength of Fano dip, the forward scattering intensity for the 75-nm-thick shell is 12-fold larger than that for no shell (0-nm-thick shell). These calculated results are consistent with the experimental results shown in Figs. 4(b) and 4(c). The experimental and calculated results shown here indicate that a strong directional Fano resonance occurs upon forming a $SiO_2$ shell that is thicker than ~40 nm.

For further analysis of the directional scattering of a $Si/SiO_2$ nanoparticle, the ratio between the forward- and backward-scattering intensities is shown in Fig. 4(f) as a function of shell thickness. The ratio is estimated from the results calculated by Eqs. (2) and (3).The red dots indicate the ratio for each shell thickness at the Fano dip. The ratio for the shell thickness of 0 nm, which means a bare Si nanoparticle, is normalized to 1.0. The ratio remains at this same level for thicknesses from 0 to 40 nm. When the shell becomes thicker than 40 nm, the ratio drastically increases up to $\sim 10^5$ at the thickness of 57 nm. This result is attributed to the backward-scattering intensity having a minimum value of $\sim 10^{-5}$ for the shell thickness of 57 nm, which is $\sim 10^4$ times less than that of the Si nanoparticle, whereas the forward-scattering ratio is nine fold larger than for no shell. We define this extremely weak backward scattering as "zero backscattering" in this paper. When the shell is more than 57 nm thick, zero backscattering is broken, resulting in the decline of the ratio. An optimum shell thickness clearly exists to achieve the highest ratio of forward-scattering to backward-scattering for $Si/SiO_2$ nanoparticles. For the $Si/SiO_2$ nanoparticle with a core diameter of 130 nm, the optimum shell thickness is 57 nm, and the ratio is five orders of magnitude greater than that of a Si nanoparticle with the same Si diameter.

We now discuss the factor that causes zero backscattering. In general, zero backscattering requires the first Kerker condition, which imposes equal electric- and magnetic-multipole coefficients ($a_n = b_n$). To check whether this condition is satisfied in the present system, it suffices to calculate the backward-scattering intensity derived from only dipole moments. In this case, Eq. (2) may be simplified to the form

$$I_B = \left(\frac{1}{4k^2}\right)\left|3\left(a_1 - b_1\right)\right|^2. \tag{6}$$

#262908 Received 12 Apr 2016; revised 14 Jun 2016; accepted 15 Jun 2016; published 17 Jun 2016
© 2016 OSA

If the first Kerker condition is satisfied, $I_B$ should be 0. The intensity was calculated at the Fano dip for the $Si/SiO_2$ nanoparticle with core diameter and shell thickness of 130 and 57 nm, respectively. The intensity, however, is much greater than zero (~$10^2$), indicating that the first Kerker condition is not satisfied in this system. Next, we consider quadrupole moments, modifying the equation as follows:

$$I_B = \left(\frac{1}{4k^2}\right)\left|5(a_2 - b_2) - 3(a_1 - b_1)\right|^2. \quad (7)$$

In this case, the intensity at the Fano dip drastically approaches to zero (~$10^{-1}$) because the quadrupole- and dipole-moment terms cancel each other out. Considering higher-order moments than quadrupoles, the intensity finally is found to be ~$10^{-4}$. This result suggests that interplay between multipoles [36] is what leads to zero backscattering for $Si/SiO_2$ nanoparticles.

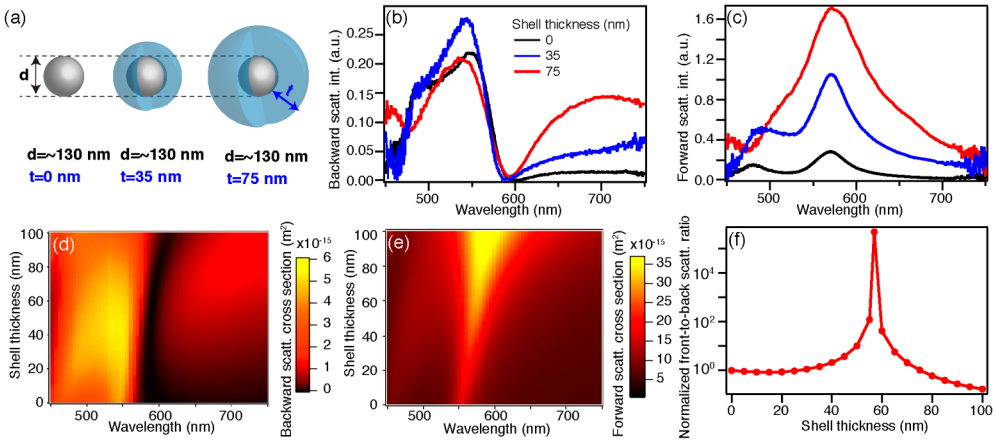


Fig. 4. (a) Schematics of $Si/SiO_2$ nanoparticles with approximately equal core diameters (~130 nm) and various shell thicknesses (0, 35, and 75 nm) (b), (c) Backward- and forward-scattering spectra of the nanoparticles illustrated in (a). (d), (e) Color maps of backward- and forward-scattering intensities from a $Si/SiO_2$ nanoparticles, respectively. The core diameter is 130 nm and the shell thickness ranges from 0 to 100 nm. (f) Front-to-back scattering-intensity ratio at the wavelength of the Fano dip for the $Si/SiO_2$ nanoparticle (core diameter: 130 nm) as a function of shell thickness. The ratio was normalized by the ratio of the Si nanoparticle (diameter: 130nm).

The influence of core diameter on the Fano resonance was also investigated experimentally and theoretically. Figure 5(a) shows schematics of experimentally used $Si/SiO_2$ nanoparticles of various core diameters (106, 130, and 142 nm) and approximately the same shell thicknesses (~75 nm). All particles were prepared by thermal oxidation of silicon nanoparticles for 240 min. Obtained backward-scattering spectra for those nanoparticles were shown in Fig. 5(b). The spectra were normalized by the intensities at the MD-resonance wavelength. Each spectrum shows a distinctive dip structure originating from the Fano resonance. The wavelengths of the dips clearly blueshift with decreasing core diameter, which indicates that the wavelength of the Fano resonance can be controlled over the entire visible region by changing the core diameter. Regarding the spectral lineshape of the Fano resonance, decreasing the core diameter enhances the intensity at the red side of the Fano dip. In other words, the asymmetric lineshape for a 142 nm core diameter gradually becomes symmetrical as the core diameter decreases. We explain this phenomenon based on another Mie-theory calculation. Figures 5(c)–5(e) show the calculated scattering cross sections of the ED and MD resonances for $Si/SiO_2$ nanoparticles with various core diameters and a fixed shell thickness. For this calculation, the core diameters are 106, 130, and 142 nm and the shell thickness is 75 nm. Here we focus on the detuning between the resonance

#262908 Received 12 Apr 2016; revised 14 Jun 2016; accepted 15 Jun 2016; published 17 Jun 2016
© 2016 OSA

wavelengths of the ED and MD resonances. For core diameters of 106, 130, and 142 nm, the detunings between the resonance wavelengths are 42, 55, and 63 nm, respectively. The detuning of the resonance wavelengths becomes small upon decreasing the core diameter, which leads to a more symmetric lineshape. Thus, in this system, decreasing the core diameter leads to a small detuning between the ED and MD resonance wavelengths and, as a result, the asymmetric line-shape approaches the symmetric lineshape. In addition, the spectral width of the MD resonance is seen to narrow as the core diameter decreases, thereby sharpening the Fano-dip structure, as also seen in the experimental results.

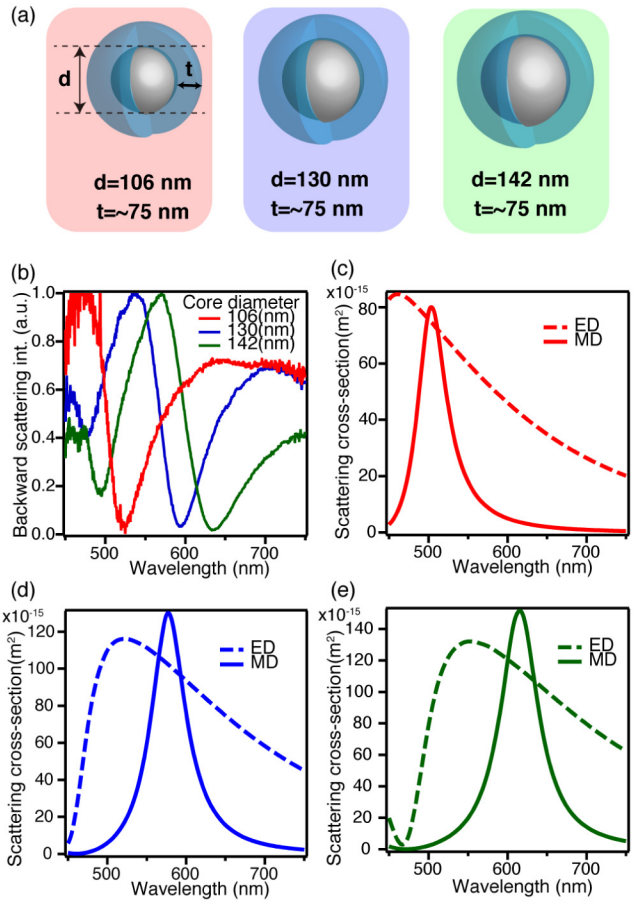


Fig. 5. (a) Schematics of $Si/SiO_2$ nanoparticles with various core diameters (106, 130, 142 nm) and approximately equal shell thicknesses (~75 nm). (b) Experimental backward-scattering spectra of those nanoparticles. (c)–(e) Calculated scattering cross-sections of ED (dashed line) and MD (solid line) resonances for $Si/SiO_2$ nanoparticles with various core diameters (106, 130, 142 nm) and a fixed shell thickness (75 nm). Red, blue, and green lines indicate the result for the core diameters of 106, 130, and 142 nm, respectively.

Finally, we investigate how the index of refraction of the surrounding medium affects the spectrum of the Fano resonance. The backward-scattering spectra of the $Si/SiO_2$ nanoparticle (core diameter 130 nm, shell thickness ~75 nm) shown in Fig. 5(a) were measured in various media with differing refractive indices ($n_s$). Figure 6(a) shows spectra of the $Si/SiO_2$ nanoparticle in air ($n_s$ = 1.00), water ($n_s$ = 1.33), and oil ($n_s$ = 1.52). All spectra are normalized by the intensities at the corresponding MD-resonance wavelength. The spectrum of the particle in air exhibits a clear Fano dip at $\lambda$ = 590 nm and high intensity at wavelengths greater than 600 nm. The intensity decreases with increasing index of refraction of the surrounding medium, leading to the disappearance of the clear dip structure. In contrast to the

#262908 Received 12 Apr 2016; revised 14 Jun 2016; accepted 15 Jun 2016; published 17 Jun 2016
© 2016 OSA

distinctive change in intensity, the wavelengths of the dips shift only by ~10 nm. Figure 6(b) shows the calculated backward-scattering spectra from the $Si/SiO_2$ nanoparticle with core diameter and shell thickness of 130 and 75 nm, respectively. The indices of refraction of the surrounding medium are 1.00, 1.33, and 1.52, which correspond to the indices of refraction of the surrounding media used experimentally. These calculated spectra are very consistent with the experimental spectra. For $Si/SiO_2$ nanoparticles, the shift in wavelength caused by the change in index of refraction of the surrounding medium is very small because the $SiO_2$ shells prohibit electric near fields from penetrating into the surrounding media [31]. When it comes to intensity, the clear change in intensity at the Fano resonance can serve in applications requiring intensity-based sensing of the index of refraction [37].

Sensitivity of a Si nanoparticle to change of a surrounding medium has been reported [38]. Here, we calculated the sensitivity of a $Si/SiO_2$ nanoparticle (core diameter 130 nm, shell thickness 75 nm). For comparison, the sensitivity of a Si nanoparticle (diameter 130 nm) was also estimated. The sensitivity was defined by the following equation:

$$Sensitivity = \frac{\partial I_B}{\partial n_s} \tag{8}$$

where $I_B$ is backward-scattering intensity calculated by Eq. (2). The wavelength used in this calculation is 700 nm where the largest intensity change is seen [Fig. 6(b)]. Figure 6(c) shows the sensitivity of the Si and $Si/SiO_2$ nanoparticle as a function of index of refraction of a surrounding medium. The sensitivity of the $Si/SiO_2$ nanoparticle indicates higher sensitivity than that of the Si nanoparticle. In particular, the difference between two particles is large at the lower index of refraction. The result indicates that the $Si/SiO_2$ nanoparticle is useful for the sensing under low index of refraction of a surrounding medium.

To understand why the Fano dip becomes unclear with increasing the index of refraction of the surrounding medium, we investigate the detuning of the ED and MD resonances and how the broadening of each resonance is affected by the surrounding index of refraction. We used Mie theory to calculate the scattering cross section of each resonance for the $Si/SiO_2$ nanoparticle. Based on the calculation, the detuning is estimated from the calculation, with the results shown in Fig. 6(d). The detuning is seen to increase by 20 nm as the surrounding index of refraction goes from 1.0 to 1.52. This increased detuning results in a small superposition of the ED and MD resonances, leading to the decreased intensity at the red side of the Fano dip, as happens in Fig. 5. The width of the scattering peak, defined as the full width at half maximum, is also estimated from the calculation and is displayed in Fig. 6(d). For the ED resonance, the peak width rapidly decreases with increasing index of refraction of the surrounding medium. In contrast to the ED resonance, the peak width of the MD resonance slightly increases. Because of these changes, the condition for interference between the narrow MD and broad ED resonance is no longer satisfied, making the Fano dip unclear in this system.

#262908 Received 12 Apr 2016; revised 14 Jun 2016; accepted 15 Jun 2016; published 17 Jun 2016
© 2016 OSA

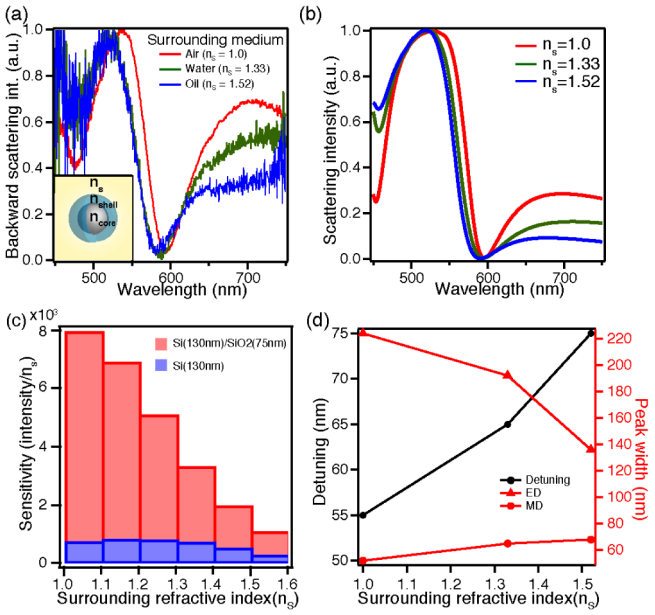


Fig. 6. (a), (b) Experimental and calculated backward-scattering spectra for a $Si/SiO_2$ nanoparticle (core diameter: 130 nm, shell thickness: 75 nm) in media of differing indices of refraction. Red, green, and blue lines indicate the spectra when the surrounding medium is air ($n_s$ = 1.0), water ($n_s$ = 1.33), and oil ($n_s$ = 1.52), respectively. The inset in (a) illustrates the $Si/SiO_2$ nanoparticle in a medium with $n_s$. (c) Sensitivity of the Si nanoparticle (diameter: 130 nm) and the $Si/SiO_2$ nanoparticle (core diameter: 130 nm, shell thickness: 75 nm) as a function of index of refraction of a surrounding medium. (d) Detuning (black line) in ED and MD resonances and peak width (red line) of ED (triangles) and MD (circles) resonances for the $Si/SiO_2$ nanoparticle.

## 4. Summary

In summary, we utilize single $Si/SiO_2$ nanoparticles to demonstrate a magnetic-based directional Fano resonance. The Fano resonance, which results from interference between the ED resonance broadened by the $SiO_2$ shells and the relatively narrow MD resonance, appears clearly in backward-scattering spectra. By changing the core diameter, the Fano resonance can be controlled over the entire visible range. For a wide range of shell thickness, the backward-scattering intensity is almost zero at the wavelength of the Fano dip. However, the forward-scattering intensity has large value and increases monotonically with increasing shell thickness. Furthermore, our calculation indicates that zero backscattering occurs at the Fano dip for a specific shell thickness, following which the ratio of front-scattering to back-scattering intensity increases five orders of magnitude with respect to that of a Si nanoparticle. Finally, the Fano lineshape is investigated as a function of the index of refraction of the surrounding medium. Changes in the index of refraction lead to slight shifts in the wavelength of the Fano resonance but to a distinctive change in the Fano lineshape.

$Si/SiO_2$ nanoparticles can be easily fabricated by thermal oxidation. Furthermore, the nanoparticles provide precise control of their electromagnetic-resonance properties just by changing their core diameter and shell thickness. This system is thus a highly promising candidate for designing low-loss nanophotonic devices such as nano-antennas, metamaterials, and refractive index sensors.


## Acknowledgments

This work was partially sponsored by Grant-in-Aid for scientific research (25286030, 26706006), and JSPS Core-to-Core Program, A. Advanced Research Networks.



#262908 Received 12 Apr 2016; revised 14 Jun 2016; accepted 15 Jun 2016; published 17 Jun 2016


© 2016 OSA